# Electric Conduction-Blocking Effects of Voids and Second Phases in Stabilized Zirconia

L. Dessemond[1], R. Muccillo[2], M. Hénault[1], M. Kleitz[1]

[1] Laboratoire d'Ionique et d'Electrochimie du Solide de l'INP de Grenoble, Associé au C.N.R.S., Domaine Universitaire, B.P. 75, F-38402 Saint Martin d'Hères Cédex, France (Fax: +33/76 82 66 70)

[2] Comissão Nacional de Energia Nuclear, Instituto de Pesquisas Energéticas e Nucleares, C.P. 11049, São Paulo 05499, Brazil

Received 18 February 1993/Accepted 11 March 1993

**Abstract.** To elucidate the conduction-blocking process observed in sintered electric ceramics, measurements have been carried out on a weld between two YSZ (Yttria-Stabilized Zirconia) single crystals and on YSZ $Al_2O_3$ composites in addition to previous measurements on cracks generated at room temperature in YSZ single crystals. A fraction of the mobile oxide ions appears to be blocked at impermeable parts of the internal surfaces. The surfaces of voids (cracks, pores, and probably parts of the grain boundaries) can generate the same blocking effects as the surface of precipitated second phases.

PACS: 81.40, 84.60

The grain boundary blocking effect in sintered zirconias (cubic, tetragonal or partially stabilized) is a well documented phenomenon [1–5] which can be described in terms of either series or parallel circuits, depending on the physics of the phenomena. For instance, the series circuit more appropriately relates the observed additional "grain boundary semicircle" to the electric properties of a blocking precipitate. On the other hand, the parallel circuit more directly describes the phenomena in terms of mobile carriers being blocked at some parts of the grain boundaries. Details on these models have been given elsewhere [6] and are summarized in Figs. 1, 2 quoted from [7].

The blocking effect can be consistently measured by the blocking factor $o_B$ defined either from admittance diagram parameters (cf. Fig. 1), by

$$o_B = \Sigma_g / \Sigma_t , \tag{1}$$

where

$$\Sigma_t = \Sigma_g + \Sigma_p , \tag{2}$$

or from impedance diagram parameters (cf. Fig. 2), by:

$$o_B = R_g / (R_b + R_g) . \tag{3}$$

It directly gives the fraction of the electric carriers being blocked at the impermeable internal surfaces, under the measuring conditions, with respect to the total number of electric carriers in the sample.

The goal of this brief paper is to report new blocking features which support the assumption of an observed blocked conductance associated with the fraction of the electric carriers being blocked at interfaces.

Measurements were performed on cracks in YSZ single crystals (YSZ: Yttria-Stabilized Zirconia), on a welding between two YSZ single crystals and on YSZ $Al_2O_3$ composites. The single crystals, kindly supplied by Crismatec, were doped with 10 mole% $Y_2O_3$. The bases on which we

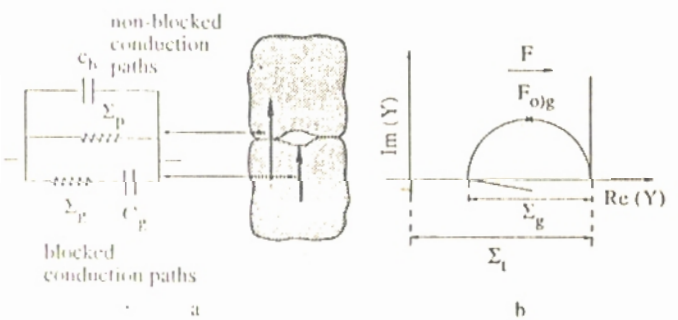


Fig. 1. Grain-boundary effect. Basic diagram of the parallel model [7]

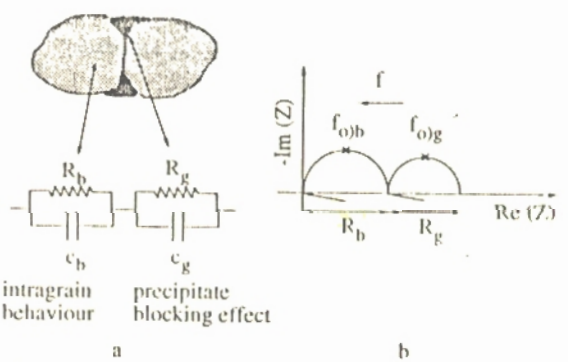


Fig. 2. Grain-boundary effect. Basic diagram of the series model [7]

worked were oriented perpendicular to the [111] direction. The zirconia–alumina composites were prepared by wet mixing of a 9 mole % yttria-stabilized zirconia powder and an alumina powder. The mixture was pressed isostatically under 400 MPa, and sintered at 2023 K for 2 h in air. After sintering the YSZ grain size was of the order of 10 µm and the alumina grain sizes were in the range 2–6 µm.

The YSZ powder was prepared from zirconia (Merck 8909) and yttria (Rhône-Poulenc, 4N) powders and the alumina was purchased from Baikovski (A125 AS3). The following compositions in $Al_2O_3$ were prepared: 0, 0.2, 0.5, 1.0, 2.0, 5.0 mole %.

The impedance measurements were performed with a Hewlett Packard HP4192 A LF impedance analyzer. The data were processed with a software that we have developed for the Hydro Quebec Research Center (IREQ) and which runs on a Hewlett-Packard 300 desk top computer.

## 1 Cracks in Single Crystals

The cell used to perform measurements on cracks and a typical admittance diagram are shown in Fig. 3.

The cracks were generated at room temperature by Vickers indentation. The measurements were conducted locally with a platinum point electrode.

The essential feature we want to stress here is the following: qualitatively, the response of the cracks is similar to that of the grain boundaries and this even at 750 K at the very start of the first temperature cycle. Under these conditions, a chemical segregation or a second-phase precipitation has certainly not yet taken place and cannot be invoked as the determining physical process. Only the geometrical mismatch between the faces of the cracks can be responsible for the blocking effect. More experimental details can be found in [6, 8].

## 2 Bicrystal Weld

Two parts of a single crystal were roughly polished on the faces to be welded with a grinding machine (roughness of the order of 1 µm), slightly pressed and welded by curing at 2273 K for 7 h. The micrography of the weld shows the presence of pores of about 10 µm in thickness [7]. Another single piece of the single crystal was subjected to the same temperature cycle for use as a reference. The admittance diagrams (Fig. 4) can be resolved into two conduction blocking characteristics. The low-frequency (LF) characteristic is very similar to that of grain boundaries. The high-frequency response (HF) can be attributed to a blocking process at the surface of the pores. This process relaxes at a frequency rather close to that of the intragrain dielectric relaxation of YSZ with which it overlaps. For greater accuracy in the deconvolution of the corresponding loops, we used the reference single crystal diagram from which we calculated the "intragrain response" of the bicrystal: the high-frequency blocking response was determined by the difference between the experimental response and this calculated "intragrain" characteristic.

With this bicrystal, the idea was to vary the bicrystal thickness $t$ (see Fig. 5a) by successive cuttings, keeping the same weld. The crystal thicknesses $t$ varies from 5.32 mm to 1.82 mm.

According to the series models, whatever the physics, segregation or precipitation, the resistances associated with

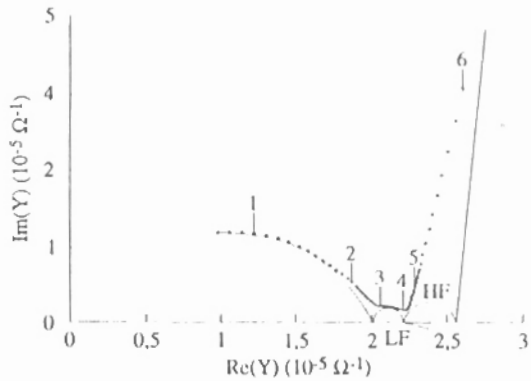


**Fig. 4.** Typical admittance diagram obtained on a weld between two single crystals at 673 K. Measurements were performed in air. The numbers indicate the ac frequency logarithm. LF and HF are the low- and high-frequency conduction blocking responses

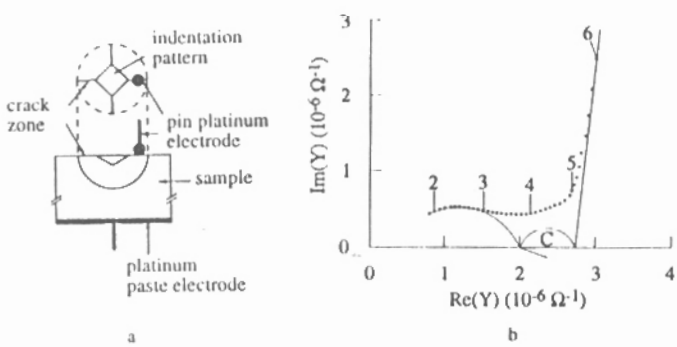


**Fig. 3.** **a** Diagram of the electrochemical cell used for local impedance spectroscopy characterisation of cracks and **b** typical admittance diagram obtained at 673 K on a single crystal indented under a 392 N load. $C$ is the crack response. Measurements were performed in air. The numbers indicate the ac frequency logarithm [7]

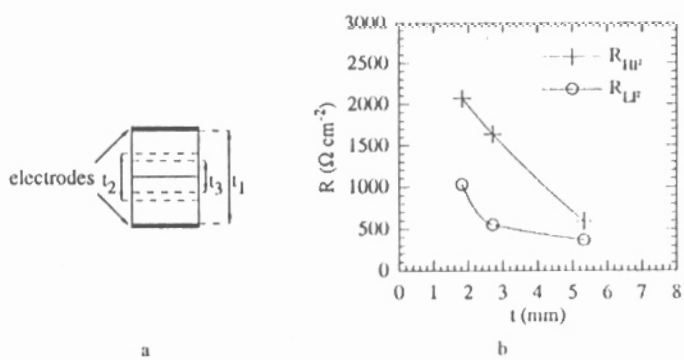


**Fig. 5.** **a** Successive cuttings of the welded bicrystal and **b** resistances per unit surface area of contact associated with the blocking processes versus the thickness of the welded bicrystal

the blocking processes at the weld should be independent from $t$. However, this is not at all the case, as shown in Fig. 5b.

## YSZ–$Al_2O_3$ Composites

With the zirconia–alumina composites, we examined the variation of the blocking effect with temperature. It is well known that the blocking effect disappears at high temperature. With nominally pure YSZ, Bernard [9] noticed that this occurs around 1000 K. In agreement with the exponential laws generally reported on Arrhenius diagrams for $N_b$ and $N_g$ (or $R_b$ and $R_g$), the general shape of the variation law for $\alpha_R$ is a sigmoïd (Fig. 6). In the central part the variation is approximately linear with temperature. This variation law allows us to define a temperature $T_t$ where $\alpha_R$ starts to decrease, and a temperature $T_d$ where the blocking effect practically disappears. With the samples investigated by Bernard [9], it was found that the higher the blocking factor, the higher the transition temperature $T_t$.

Figures 7a–c show the linear parts of the variations observed with different $Al_2O_3$ contents. Table 1 gives the corresponding equations and the temperatures $T_d$ at which the blocking effect practically disappears. The $Al_2O_3$ solubility in YSZ is generally assumed to be of the order of 0.4 mole % at 2000 K [9, 10]. The remarkable feature is that the slope of the $\alpha_R$ decrease versus $T$ (Table 1) does not show any significant differences between samples with low alumina contents, which could dissolve into the zirconia grains, and those with high concentrations which certainly cannot. Obviously, the disappearance of the blocking effect cannot be related to the dissolution of the second phase present in the material. The temperatures $T_d$ of the disappearance of the blocking effect (Table 1) are also far too low to be interpreted in this way.

At this stage, the only interpretation which appears realistic is that the volume of the blocked zones, similar to space-charges, in contact with the alumina grains, decreases with increasing temperature because of an increasing conductivity of the YSZ. It is a common observation in semiconductors, for instance, that space-charge effects decrease with increasing conductivity. In fact, variations in the degree of charge carrier blocking have also been observed in electronic conductors, for instance in $BaTiO_3$ [11]. A rather general observation is that, in reasonably pure materials, blocking at grain boundaries disappears when the conductivity reaches approximately $10^{-4}\ \Omega^{-1}\mathrm{cm}^{-1}$, whatever it is, electronic or ionic.

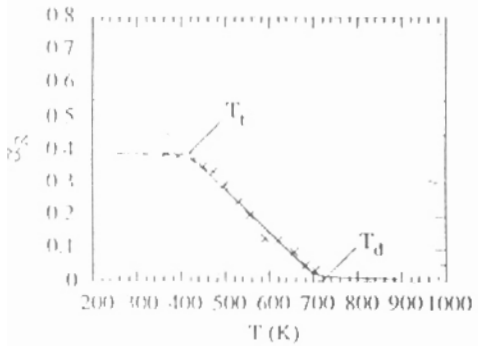


Fig. 6. Blocking factor vs temperature for YSZ (X: experimental results; —: approximated curve showing a linear decrease between $T_t$ and $T_d$)

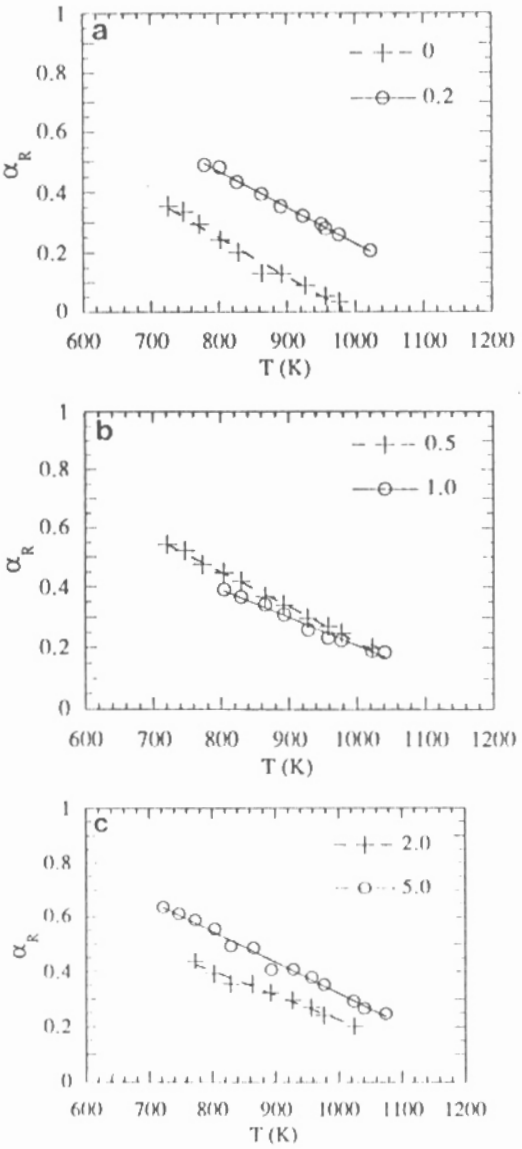


Fig. 7. Blocking factor vs temperature for YSZ $Al_2O_3$ composites (*linear parts*). The compositions in $Al_2O_3$ marked in the diagrams are in mole %

Table 1. Parameters of the linear variation of the blocking factor as a function of temperature for different YSZ $Al_2O_3$ composites. $T_d$: temperatures at which the blocking effect pactically disappears

| $Al_2O_3$ [mole %] | $\alpha_R = A - (B \cdot T[K])$ | | $T_d$ [K] |
|---|---|---|---|
| | $A$ | $B$ [$10^{-4}$ K$^{-1}$] | |
| 0 | 1.30 | 1.31 | 949 |
| 0.2 | 1.42 | 1.19 | 1193 |
| 0.5 | 1.38 | 1.16 | 1190 |
| 1.0 | 1.13 | 0.92 | 1228 |
| 2.0 | 1.10 | 0.88 | 1250 |
| 5.0 | 1.45 | 1.13 | 1283 |

## 4 Conclusion

Experimental results obtained with bicrystals and zirconia - alumina composites support the assumption that the observed blocking effect in stabilized zirconia results directly from the formation of blocked zones, where electric carriers are "trapped" and do not contribute to the transport of the electric current, under certain experimental conditions. This effect decreases as the conductivity of the matrix increases. The blocked zones are formed along internal surfaces impermeable to the electric carriers. Such impermeable internal surfaces may simply be the interfaces with a precipitated second phase. The results obtained with cracks and pores show that the surfaces of voids can also be impermeable to the electric carriers. Accordingly, the blocking effect observed at the grain boundaries could also result from local mismatches between grains.

This derivation does not discard possible additional resistances associated with a segregation of yttrium or impurities. It simply stresses that blocking of a fraction of the mobile ions at internal surfaces impermeable to them is an important contribution to the observed grain boundary effect.

In agreement with this interpretation, the experimental results are better expressed in terms of any parameter which measures the concentration of blocked ions than in terms of any "additional" resistance. For the same reason, it is better modeled in terms of parallel rather than series circuits.

## References


1. S.P.S. Badwal, J. Drennan, A.E. Hughes: In *Science of Ceramic Interfaces*, ed. by J. Nowotny (Elsevier, Amsterdam 1991) pp. 227–284
2. B.C.H. Steele: In *High Conductivity Solid Ionic Conductors*, ed. by T. Takahashi (World Scientific, Singapore 1989) pp. 402–416
3. R. Gerhardt, A.S. Nowick: J. Am. Ceram. Soc. **69**, 641 (1986)
4. M.J. Verkerk, B.J. Middelhuis, A.J. Burggraaf: Solid State Ion. **6**, 159 (1982)
5. M. Kleitz, H. Bernard, E. Fernandez, E. Schouler: In *Science and Technology of Zirconia, Advances in Ceramics*, Vol. 3 (Am. Ceram. Soc., Colombus 1981) pp. 310–336
6. M. Kleitz, C. Pescher, L. Dessemond: Zirconia V, Melbourne, August 1992 (to be published in the Proceedings)
7. L. Dessemond: Impedance Spectroscopy of Cracks in Cubic Zirconia. Thesis, Grenoble (1992)
8. L. Dessemond, J. Guindet, A. Hammou, M. Kleitz: *Proc. 2nd Int'l Symp. Solid Oxide Fuel Cells*, ed. by F. Grosz et al. (CEC, Luxembourg 1991) pp. 409–416
9. H. Bernard: Microstructure and Conductivity of Sintered Stabilized Zirconia. Thesis, Grenoble (1980)
10. M. Miyayama, H. Yanagida, A. Asada: Am. Ceram. Soc. Bull. **64**, 660 (1985)
11. F. Batllo: Granulometry and Non Stoichiometry in $BaTiO_3$. Thesis, Dijon (1987)